

PLANT SCIENCE

Florigen sequestration in cellular membranes modulates temperature-responsive flowering

Hendry Susila¹, Snejzana Jurić^{1,2}, Lu Liu^{3,4}, Katarzyna Gawarecka¹, Kyung Sook Chung¹, Suhyun Jin¹, Soo-Jin Kim¹, Zeeshan Nasim¹, Geummin Youn¹, Mi Chung Suh⁵, Hao Yu³, Ji Hoon Ahn^{1*}

Plants respond to temperature changes by modulating florigen activity to optimize the timing of flowering. We show that the *Arabidopsis thaliana* mobile florigen FLOWERING LOCUS T (FT) interacts with the negatively charged phospholipid phosphatidylglycerol (PG) at cellular membranes and binds the lipid bilayer. Perturbing PG biosynthesis in phloem companion cells leads to temperature-insensitive early flowering. Low temperatures facilitate FT sequestration in the cellular membrane of the companion cell, thus reducing soluble FT levels and delaying flowering. A mutant in *PHOSPHATIDYLGLYCEROLPHOSPHATE SYNTHASE 1* accumulates more soluble FT at lower temperatures and exhibits reduced temperature sensitivity. Thus, cellular membranes sequester FT through their ability to bind the phospholipid PG, and this sequestration modulates the plant's response to temperature changes.

Plants improve their ability to survive and reproduce by monitoring ambient temperatures and modulating the complex signaling cascades that regulate growth and development (1, 2). In particular, plants regulate flowering by integrating various environmental cues and endogenous signals. The transition from vegetative to reproductive growth is initiated in the leaves, which perceive floral-promoting signals such as day length. Leaf cells produce florigen, a conserved, long-distance flowering activator that is transported to the shoot apical meristem, where it activates the plant's re-

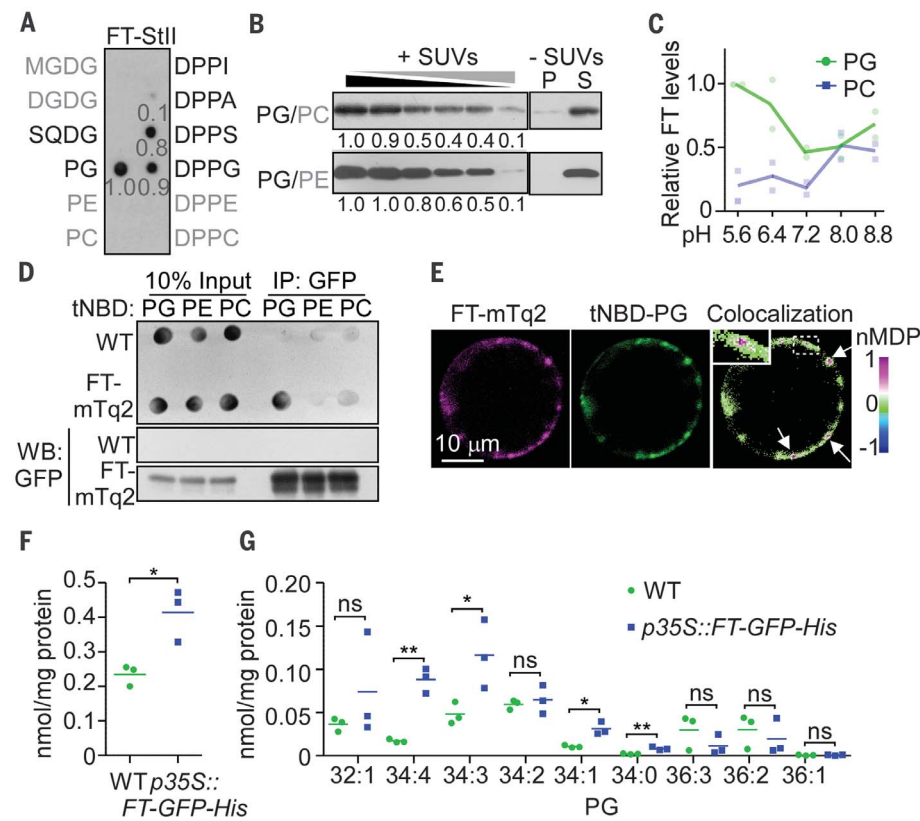
productive program. Modulation of florigen transport and activity in response to changes in ambient temperature affects crop growth. In this study, we investigated how intracellular lipid membranes regulate the transport of florigen.

To determine the lipid-binding capabilities of the florigen molecule, we tested the interaction of *Arabidopsis thaliana* FLOWERING LOCUS T (FT) (3) with phospholipids and galactolipids. FT preferentially interacted with negatively charged phospholipids, showing the strongest interaction with phosphatidylglycerol (PG) (Fig. 1A and fig. S1, A and B). Recombinant

His-FT was pulled down with PG and phosphatidylserine (PS) in vitro (fig. S1C). Testing the binding of recombinant His-tagged FT to small unilamellar vesicles (SUVs) showed that the SUVs that were composed of 100% PG efficiently sedimented FT, whereas increasing the proportion of the neutral phospholipids phosphatidylcholine (PC) and phosphatidylethanolamine (PE) reduced FT sedimentation (Fig. 1B and fig. S1, D and E). We observed preferential binding of His-FT to PG rather than PC at acidic and neutral pH conditions (Fig. 1C and fig. S1F), which correspond to the pH of most intracellular compartments (4). The dissociation constant (K_d) value of the FT-PG interaction was $1.6 \pm 0.9 \mu\text{M}$; we failed to obtain a K_d value for the FT-PC pair, consistent with the preferential binding of FT to PG (fig. S1G).

We then turned to protein-lipid reciprocal coimmunoprecipitation assays in *Arabidopsis* protoplasts to assess whether FT binds phospholipids in vivo. Indeed, FT fused to the fluorescent protein mTurquoise2 (FT-mTq2)

Fig. 1. Phospholipid-binding properties of FT. (A) Lipid overlay assay of recombinant FT fused to Strep-tag II (FT-StII) with various phospholipids and galactolipids. Black, negatively charged; gray, neutral (for further explanation and definition of abbreviations, see materials and methods). (B) Liposome binding assay of recombinant His-FT with different combinations of PG/PC and PG/PE SUVs. Sedimentation with 100% PG SUVs was set to 1.0. P, pellet; S, supernatant. (C) Relative FT levels, as detected with anti-His antibodies, from liposome binding assays using PG or PC SUVs at different pH levels. Recombinant His-FT levels with PG SUVs at pH 5.6 were set to 1.0. (D) In vivo protein-phospholipid coimmunoprecipitation assays using FT-mTq2 and tNBD-phospholipids in protoplasts. WT, wild type; WB, western blot; GFP, green fluorescent protein; IP, immunoprecipitation. (E) Colocalization of FT-mTq2 (magenta) and tNBD-PG (green) in protoplasts. Color scale, normalized mean deviation product (nMDP) from signal intensity in colocalization heatmap; arrows, colocalization spots. (F and G) Quantification of PG levels (F) and PG molecular species (G) coimmunoprecipitated by FT-GFP-His with LC-MS/MS. Asterisks represent significant differences derived from Student's *t* tests (ns, nonsignificant; * $P \leq 0.05$, ** $P \leq 0.01$).



interacted with PG in vivo (Fig. 1D and fig. S1H). This is consistent with the finding that FT-mTq2 colocalized with 16:0-12:0 c7-nitro-1,2,3-benzoxadiazole-PG (tNBD-PG) in protoplasts (Fig. 1E, arrows, and fig. S2). Consistent with these observations, liquid chromatography-tandem mass spectrometry (LC-MS/MS) and ultra-performance liquid chromatography-electrospray ionization-tandem mass spectrometry (UPLC-ESI-MS/MS) analyses showed that, compared with other phospholipids, more PG (especially PG 34:4 and PG 34:3) coimmunoprecipitated with FT-GFP-His in *p35S::FT::GFP::His* plants in vivo (Fig. 1, F and G and fig. S3). We also tested the phospholipid binding potential of *Arabidopsis* FT homologs by using recombinant proteins with a His tag. As shown with FT, increasing the relative amount of PE reduced sedimentation of *Arabidopsis* FT homologs with PG SUVs (fig. S4). Thus, FT and FT-related proteins prefer to bind to PG in vitro and in vivo, which contradicts a previous report (5). This discrepancy is likely due to differences in experimental conditions, including pH (Fig. 1C) and PG molecular species used.

We next examined the intracellular localization of FT and its behavior at intracellular membranes. We observed localization of FT in TERMINAL FLOWER 1-related vesicles (dense, 100-nm vesicles that may be associated with trafficking to the protein storage vacuole) (6), as well as the outer envelope of free chloroplasts (Fig. 2A), consistent with the finding that the chloroplast envelope is rich in PG (7), in addition to the other organelles in which FT localizes (8–10) (fig. S5A). We confirmed the localization of FT in the chloroplast outer envelope by immunogold labeling experiments (fig. S5B). The PG-binding lipopeptide daptomycin, which competitively binds to PG, reduced FT binding to the chloroplast envelope

(fig. S5C). By contrast, FT showed little colocalization with the mitochondria or multivesicular bodies (i.e., prevacuolar compartments) (Fig. 2B and fig. S5D). These results suggest that FT localizes to some—but not all—types of intracellular membrane compartments in vivo.

We next incubated purified thylakoids with recombinant FT to investigate how FT behaves at the PG-rich thylakoid membrane (7). FT was not washed away by alkaline (urea and Na₂CO₃) or chaotropic (NaCl and NaSCN) agents and was instead found in the pellet (Fig. 2C and fig. S6A), similar to the thylakoid transmembrane protein CURVATURE THYLAKOID 1A (II), suggesting that FT is likely buried in the membrane, similar to its putative bovine homolog (12). By contrast, recombinant FT proteins harboring the Arg¹¹⁹→His (R119H) or Pro⁹⁴→Leu (P94L) substitutions, characteristic of the *ft-3* and *ft-6* mutants (13, 14), respectively, were washed off of the membrane by alkaline and chaotropic agents, although they retained the ability to bind phospholipids (fig. S6, A to C), similar to the peripheral thylakoid protein NAD(P)H DEHYDROGENASE SUBUNIT H (II). The *ft-3* and *ft-6* proteins do not interact with the FT binding partners FD and 14-3-3 (GENERAL REGULATORY FACTOR3) (fig. S6D) (8, 15), suggesting that the *ft-3* and *ft-6* proteins are unable to form the florigen activation complex (15) in the shoot apical meristem. As the R119 and P94 residues sustain the integrity of the anion binding pocket in FT (16), these data suggest that the conserved anion binding pocket is involved not only in the transcriptional activity of FT in the shoot apical meristem (17) but also in membrane binding activity.

To investigate the effects of impaired biosynthesis of PG in planta, we analyzed the flowering time of several PG biosynthesis mutants under long-day (LD) conditions. PG is synthesized mainly in the chloroplast by means of a

pathway that involves several enzymes (fig. S7A). PG biosynthesis mutants (fig. S7B) (18–20), especially those lacking PHOSPHATIDYLGLYCEROLPHOSPHATE SYNTHASE 1 (PGP1) activity, flowered earlier than their parental wild type when grown at 16°C under LD conditions (Fig. 3A and table S1, experiments 1 to 5), indicating that the mutations reduced sensitivity to temperature changes and limited the extent to which lower temperatures delay flowering (Fig. 3B). We observed no flowering time phenotype for PG biosynthesis mutants grown under short-day conditions (table S1, experiments 6 and 7). Indeed, treatment with exogenous PG—but not PC and PE—delayed flowering of wild-type and *pgp1* mutants in a dose-dependent manner (table S1, experiments 8 to 13, and fig. S8).

Although the PG biosynthesis mutants flowered early, transcript levels of *FT*, *TWIN SISTER OF FT* (*TSF*), and *SUPPRESSOR OF OVER-EXPRESSION OF CONSTANS 1* showed little change in these mutants relative to the wild type (fig. S9A). However, early flowering of *pgp1* mutants was suppressed by the *ft-10* and *ft-10 tsf-1* mutations (Table 1, experiments 1 and 2, and fig. S9, B and C), raising the possibility that the early flowering phenotype caused by a defect in PG biosynthesis might be associated with the regulation of FT proteins. We therefore investigated whether the loss of PGP1 alters the intracellular localization of FT. In wild-type plants grown under LD at 16°C, FT-9×myc was more abundant in the membrane fractions [P8 (nucleus, mitochondria, and chloroplast) and P100 (plasma membrane, endoplasmic reticulum, and small vesicles)], concomitant with a twofold reduction of FT in the soluble fraction (S100: cytosol and soluble proteins), when compared with plants grown at 23°C (Fig. 3C and fig. S10). However, *pgp1* mutants grown at 16°C accumulated less FT-9×myc in the

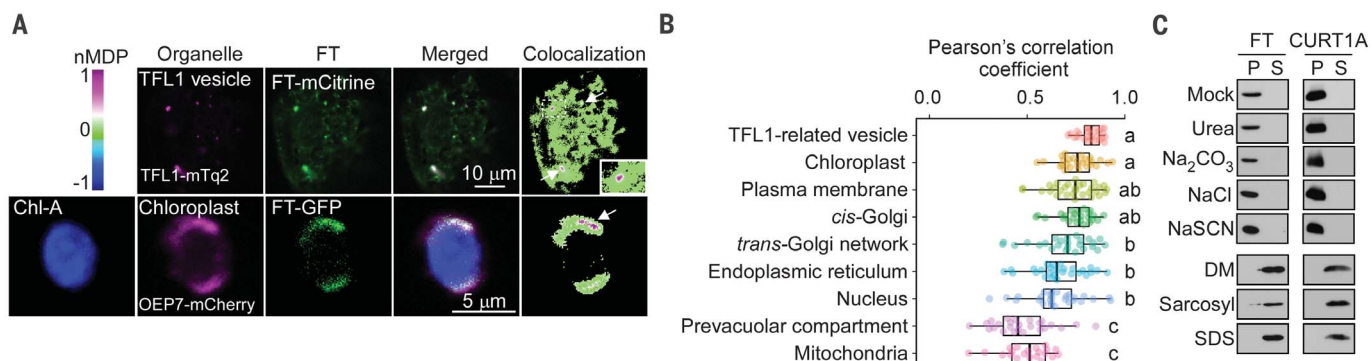
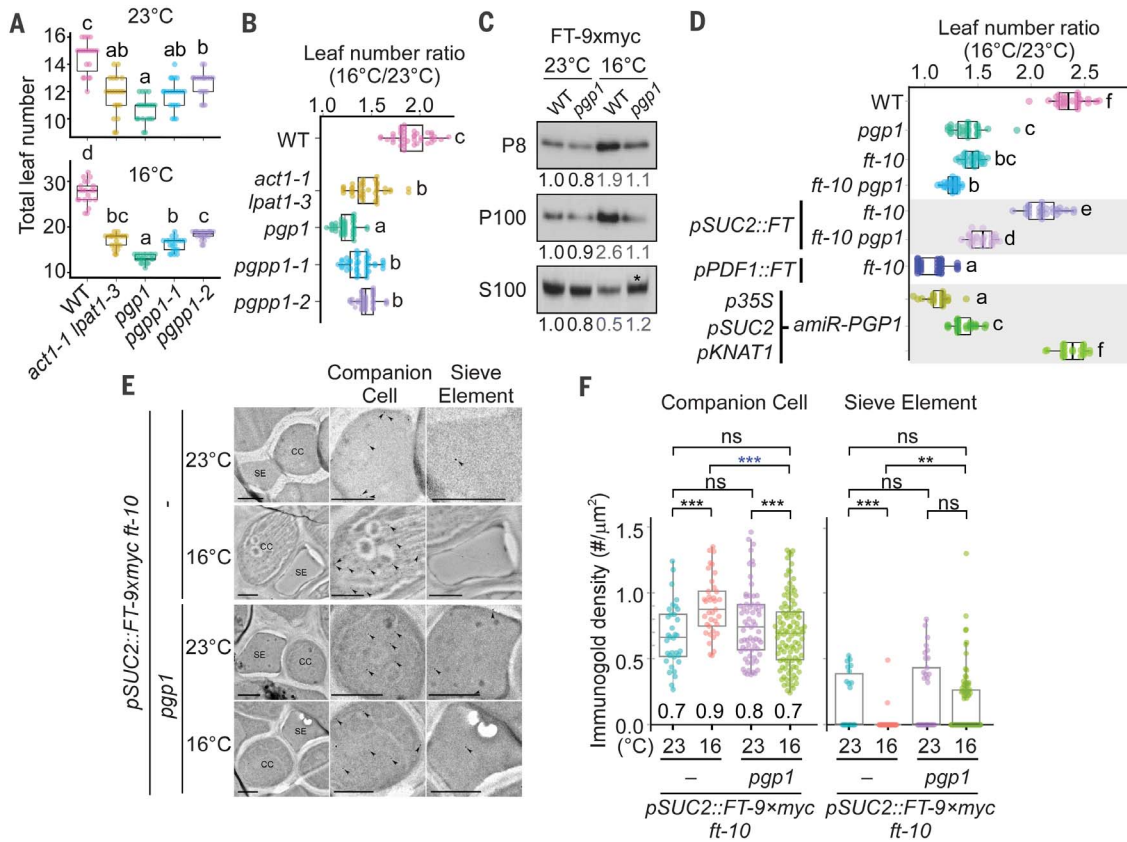


Fig. 2. FT binds the lipid bilayer of intracellular membranes. (A) Localization of FT-mCitrine (green) in TERMINAL FLOWER 1 (TFL1)-related vesicles (6) and the outer chloroplast envelope in protoplasts (mTq2-tagged membrane marker, magenta). To visualize vesicles, protoplasts were fixed with paraformaldehyde. Free chloroplasts were isolated after shearing of protoplasts to prevent a false signal from the cytosol. Color scale, nMDP from signal intensity; arrows, colocalization spots.

(B) Quantification of colocalization of FT with intracellular membrane compartments. Different lowercase letters represent significant differences derived from a one-way analysis of variance (ANOVA) followed by Tukey's multiple comparison tests ($P \leq 0.01$). (C) Chemical washing experiment of His-FT binding to the thylakoid as a model membrane. CURVATURE THYLAKOID 1A (CURT1A, thylakoid transmembrane protein) was used as a control. DM, *n*-dodecyl β-D-maltoside.

Fig. 3. Temperature and PG modulate long-distance transport of FT. (A and B) Total leaf number (A) and leaf number ratio (LNR) (B) of wild-type and PG biosynthesis mutants grown under long-day conditions. (C) Effect of the *pgp1* mutation on the intracellular distribution of FT in different cellular compartments of *ft-10 pSUC2::FT-9×myc* plants. (D) LNR of *ft-10 pgp1*, *pSUC2::FT-9×myc* plants and transgenic plants expressing *amiR-PGP1* under the control of different promoters. Different lowercase letters represent significant differences derived from a one-way ANOVA followed by Tukey's multiple comparison tests ($P \leq 0.01$). (E) Effect of the *pgp1* mutation on FT-9×myc distribution in companion cells (CC) and sieve elements (SE) in the first rosette leaf of 11-day-old *ft-10 pSUC2::FT-9×myc* seedlings, as determined by immunogold labeling. Arrowheads point to the gold particles. Scale bars, 1 μm . (F) Numbers of FT-9×myc immunogold particles in companion cells and sieve elements. Values are the average density of gold particles per square micrometer from at least 20 sections. Asterisks represent significant differences derived from Student's *t* tests (ns, nonsignificant; ** $P \leq 0.01$, *** $P \leq 0.001$).



membrane fractions, with FT-9×myc being enriched in the soluble fraction instead (Fig. 3C, asterisk). Further analyses showed that the sequestration of FT in the membrane of the chloroplast envelope, vesicles, and trans-Golgi network at 16°C is PG dependent (figs. S11 and S12). These findings suggest that impairment of PG biosynthesis reduces FT sequestration in intracellular membranes at low temperatures, leading to increased FT abundance in the soluble fraction and thus mimicking the FT distribution at higher temperatures. Consistent with this observation, endogenous PG levels were reduced in *pgp1* mutants at 23° and 16°C (fig. S13A). However, the levels of total PG in whole seedlings, P8, or P100 fractions were unperturbed by temperature (fig. S13, A and B). Ambient temperatures instead modulated the saturation levels of PG species (for instance, 34:4 and 36:6) (fig. S13C) (27). Spatial and temporal lipidomics analyses will be necessary to test the link between membrane sequestration of FT and the desaturation levels of PG species.

Our genetic analysis indicated that PG participates in the photoperiodic pathway alongside florigen. To clarify the role of PG in florigen-induced flowering, we misexpressed

FT in companion cells of the leaf vasculature with the *SUCROSE-PROTON SYMPORTER 2* promoter (*pSUC2::FT-9×myc*) or in the shoot epidermis with the *PROTODERMAL FACTOR 1* promoter (*pPDF1::FT-9×myc*). Both transgenes suppressed late flowering of *ft-10* mutants; in particular, the *pPDF1::FT-9×myc* plants showed a strong early flowering phenotype (Table 1, experiments 3 and 4, and fig. S14A). However, only *pSUC2::FT-9×myc* plants exhibited temperature-sensitive flowering [leaf number ratio (LNR); 2.1; wild type; 2.3] (22), although *FT* mRNA and FT protein levels at both temperatures were similar in *pSUC2::FT-9×myc* plants (fig. S14, B and C). Introduction of *pSUC2::FT-9×myc* in the *pgp1* mutant background caused temperature-insensitive flowering (LNR: 1.5) (Fig. 3D), similar to that seen in *pgp1* mutants (LNR: 1.4). Plants expressing FT fused with smaller tags [hemagglutinin (HA) and the 11-amino acid T7 epitope] showed similar results (table S1, experiments 14 to 16, and fig. S15) (23). In addition, knockdown of *PGP1* expression specifically in the leaf vasculature by artificial miRNA (amiR) technology (24) (*pSUC2::amiR-PGP1*) (fig. S16) resulted in early flowering at 16°C relative to the wild type

(Table 1, experiments 3 and 4) and reduced temperature sensitivity (LNR: 1.3), similar to the *pgp1* mutants (Fig. 3D). However, expressing *amiR-PGP1* specifically in the shoot apical meristem from the *KNOTTED-LIKE FROM ARABIDOPSIS THALIANA* promoter (*pKNAT1::amiR-PGP1*) did not accelerate flowering (LNR: 2.2) (fig. S16). These results indicated that PG likely acts in the leaf vasculature to modulate flowering.

We then micrografted cotyledons (fig. S17A) onto *ft-10* seedlings to test the export of florigen from micrografted cotyledons. We discovered that cotyledons with the *pgp1* mutation (*pgp1 p35S::FT-GFP-His > ft-10*) accelerated flowering of recipient *ft-10* plants compared with cotyledons with functional PGP1 at 16°C (Table 1, experiments 5 and 6, and fig. S17, B and C). The specific ablation of chloroplasts in companion cells of the leaf vasculature using amiRNAs targeting *PLASTID TRANSCRIPTIONALLY ACTIVE 10 (PTAC10)* or *CHLORINA42/SULFUR (SUL)* resulted in early flowering at 16°C with decreased LNR values (table S1, experiments 17 and 18), without affecting *FT* transcript levels (fig. S18). Together, these findings suggest that the transport of FT from the leaf is PG

Table 1. Flowering times of mutants and transgenic plants. RLN, rosette leaf number; CLN, cauline leaf number; TLN, total leaf number; Stdev, standard deviation; *n*, number of plants analyzed; #, identifier of individual transgenic lines. Different lowercase letters represent significant differences derived from a one-way ANOVA followed by Tukey's multiple comparison tests ($P \leq 0.01$).

Genotype	RLN	CLN	TLN	TLN Stdev	TLN range	<i>n</i>	$P \leq 0.01$
Experiment 1 (23°C long days)							
Col-0 (wild type)	11.3	3.1	14.4	1.3	13–17	16	b
<i>pgp1</i>	8.4	2.0	10.4	1.4	9–12	16	a
<i>ft-10</i>	30.7	7.5	38.2	3.1	36–44	16	d
<i>ft-10 pgp1</i>	28.0	6.2	34.2	2.4	29–37	15	c
<i>ft-10 tsf-1</i>	46.8	13.3	60.1	2.6	55–64	10	e
<i>ft-10 tsf-1 pgp1</i>	46.4	11.5	57.9	2.6	53–62	11	e
Experiment 2 (16°C long days)							
Col-0 (wild type)	27.0	7.1	34.1	1.7	30–36	15	b
<i>pgp1</i>	11.9	2.3	14.2	1.2	11–16	16	a
<i>ft-10</i>	36.0	7.7	43.4	3.0	39–49	13	d
<i>ft-10 pgp1</i>	31.0	6.9	37.9	2.7	34–42	15	c
<i>ft-10 tsf-1</i>	48.6	12.3	60.9	3.6	54–66	15	e
<i>ft-10 tsf-1 pgp1</i>	50.4	9.9	60.3	2.9	56–64	12	e
Experiment 3 (23°C long days)							
Col-0 (wild type)	10.5	3.0	13.5	1.0	12–16	13	e
<i>pgp1</i>	8.5	2.1	10.6	0.8	9–12	12	cd
<i>ft-10</i>	28.3	5.9	34.2	2.2	31–38	12	h
<i>ft-10 pgp1</i>	26.1	6.1	32.2	1.6	30–36	14	g
<i>pSUC2::FT:9xmyc ft-10</i>	12.1	3.8	15.9	1.0	14–17	15	f
<i>pSUC2::FT:9xmyc ft-10 pgp1</i>	10.5	3.6	14.1	0.8	13–15	13	e
<i>pPDF1::FT:9xmyc</i>	4.3	1.1	5.4	0.5	5–6	15	a
<i>35S::amiR-PGP1 #3-2</i>	7.1	1.5	8.6	0.8	7–10	11	b
<i>35S::amiR-PGP1 #6-1</i>	7.3	1.7	9.0	0.7	8–10	12	bc
<i>pSUC2::amiR-PGP1 #1-2</i>	8.1	2.5	10.6	1.0	9–12	12	cd
<i>pSUC2::amiR-PGP1 #2-1</i>	9.1	2.5	11.6	0.7	10–12	13	d
<i>pKNAT1::amiR-PGP1 #4-4</i>	9.9	2.7	12.6	0.7	12–14	12	e
<i>pKNAT1::amiR-PGP1 #9-6</i>	10.1	2.9	13.0	0.8	12–14	12	e
Experiment 4 (16°C long days)							
Col-0 (wild type)	25.6	6.1	31.7	1.8	29–35	13	ef
<i>pgp1</i>	12.8	2.7	15.5	1.1	14–17	12	c
<i>ft-10</i>	40.3	9.0	49.3	2.4	45–53	13	h
<i>ft-10 pgp1</i>	32.8	7.6	40.4	1.7	37–42	13	g
<i>pSUC2::FT:9xmyc ft-10</i>	25.3	8.3	33.6	2.3	29–37	13	f
<i>pSUC2::FT:9xmyc ft-10 pgp1</i>	16.0	5.6	21.6	1.5	19–23	14	d
<i>pPDF1::FT:9xmyc</i>	5.1	0.7	5.8	0.8	5–7	17	a
<i>35S::amiR-PGP1 #3-2</i>	8.4	1.4	9.8	0.6	8–10	11	b
<i>35S::amiR-PGP1 #6-1</i>	8.6	1.6	10.2	0.6	9–11	12	b
<i>pSUC2::amiR-PGP1 #1-2</i>	13.5	3.5	17.0	1.1	15–19	10	c
<i>pSUC2::amiR-PGP1 #2-1</i>	12.6	3.1	15.7	1.4	14–18	11	c
<i>pKNAT1::amiR-PGP1 #4-4</i>	23.9	6.0	29.9	1.5	27–32	11	e
<i>pKNAT1::amiR-PGP1 #9-6</i>	23.9	5.5	29.4	1.9	26–32	11	e
Experiment 5 (23°C long days) (donor > recipient)							
<i>ft-10 > ft-10</i>	38.9	7.9	46.8	2.3	43–51	17	c
Col-0 (wild type) > <i>ft-10</i>	29.3	6.8	36.1	2.7	31–40	11	b
<i>pgp1 > ft-10</i>	27.2	7.7	34.9	1.7	32–37	10	b
<i>35S::FT:GFP:His > ft-10</i>	22.5	7.1	29.6	4.2	27–35	16	a
<i>35S::FT:GFP:His pgp1 > ft-10</i>	19.9	6.8	26.7	3.7	20–32	12	a
Experiment 6 (16°C long days) (donor > recipient)							
<i>ft-10 > ft-10</i>	42.1	9.6	51.7	2.6	48–55	11	d
Col-0 (wild type) > <i>ft-10</i>	35.3	7.8	43.1	3.6	37–48	12	c
<i>pgp1 > ft-10</i>	32.9	6.3	39.2	3.7	35–47	10	bc
<i>35S::FT:GFP:His > ft-10</i>	31.2	7.5	38.7	7.3	26–46	13	b
<i>35S::FT:GFP:His pgp1 > ft-10</i>	23.0	6.1	29.1	2.5	25–32	10	a

dependent and that PG in leaf companion cells restricts the long-distance transport of FT.

We then performed immunogold labeling to visualize the effect of PG on FT localization in the leaf vasculature. We determined that FT-9 \times myc is more abundant (33% increase) in the companion cells of *ft-10 pSUC2::FT-9 \times myc* plants grown at 16°C than at 23°C (Fig. 3, E and F). However, introduction of the *pgp1* mutation caused a 22% decrease in FT-9 \times myc particle density in companion cells at 16°C. Among sieve elements, we observed only 2 out of 33 sieve elements with FT-9 \times myc particles from *ft-10 pSUC2::FT-9 \times myc* plants grown at 16°C. The introduction of the *pgp1* mutation raised the frequency of FT-9 \times myc particles in sieve elements at 16°C (37 out of 92 sieve elements), which was thus comparable to that seen in *ft-10 pSUC2::FT-9 \times myc* plants at 23°C (Fig. 3F). Early flowering of *pgp1* mutants at 16°C was not suppressed by a mutation in *FT-INTERACTING PROTEIN 1 (ftip1-1)* (table S1, experiments 19 and 20), suggesting that the transport of FT in *pgp1* mutants is mediated by an FTIP1-independent mechanism. These findings suggest that FT transport from companion cells to sieve elements occurs in a PG-dependent manner.

Our results demonstrate that FT interacts with the negatively charged phospholipid PG. Low ambient temperature promotes sequestration of FT within intracellular membranes in a PG-dependent manner, thereby restricting translocation of FT from companion cells to sieve elements to prevent precocious flowering. We propose that in addition to the FT-PC interaction in the shoot apical meristem that

promotes flowering (5), PG-enriched membrane domains serve as docking sites for FT proteins, thus delaying flowering under unfavorable conditions such as low temperature and providing an additional layer of regulation during florigen transport. Our results further suggest that membranes sense and adapt to external temperatures and modulate the amount of membrane-bound florigen accordingly. Because FT-like florigen proteins have conserved functions across plant species (25), sequestration of FT in membranes might serve as a common strategy for plants to adjust the timing of flowering in response to changing seasonal temperatures.

REFERENCES AND NOTES

- M. Legris, C. Nieto, R. Sellaro, S. Prat, J. J. Casal, *Plant J.* **90**, 683–697 (2017).
- H. Susila, Z. Nasim, J. H. Ahn, *Int. J. Mol. Sci.* **19**, 3196 (2018).
- L. Corbesier et al., *Science* **316**, 1030–1033 (2007).
- J. Shen et al., *Mol. Plant* **6**, 1419–1437 (2013).
- Y. Nakamura et al., *Nat. Commun.* **5**, 3553 (2014).
- E. J. Sohn et al., *Proc. Natl. Acad. Sci. U.S.A.* **104**, 18801–18806 (2007).
- P. Moreau et al., *Prog. Lipid Res.* **37**, 371–391 (1998).
- M. Abe et al., *Science* **309**, 1052–1056 (2005).
- L. Liu, C. Li, Z. W. N. Teo, B. Zhang, H. Yu, *Plant Cell* **31**, 2475–2490 (2019).
- L. Liu et al., *PLOS Biol.* **10**, e1001313 (2012).
- U. Armbruster et al., *Plant Cell* **25**, 2661–2678 (2013).
- B. S. Vallée et al., *Eur. J. Biochem.* **268**, 5831–5841 (2001).
- M. Koornneef, C. J. Hanhart, J. H. van der Veen, *Mol. Gen. Genet.* **229**, 57–66 (1991).
- Y. Kobayashi, H. Kaya, K. Goto, M. Iwabuchi, T. Araki, *Science* **286**, 1960–1962 (1999).
- K. Taoka et al., *Nature* **476**, 332–335 (2011).
- J. H. Ahn et al., *EMBO J.* **25**, 605–614 (2006).
- W. W. H. Ho, D. Weigel, *Plant Cell* **26**, 552–564 (2014).
- H. U. Kim, P. Vijayan, A. S. Carlsson, L. Barkan, J. Browse, *Plant Physiol.* **153**, 1135–1143 (2010).
- C. Xu et al., *Plant Physiol.* **129**, 594–604 (2002).
- Y.-C. Lin, K. Kobayashi, C.-H. Hung, H. Wada, Y. Nakamura, *Plant J.* **88**, 1022–1037 (2016).
- Q. Li et al., *Plant Cell* **27**, 86–103 (2015).
- L. Liu, Y. Zhang, H. Yu, *J. Integr. Plant Biol.* **62**, 1385–1398 (2020).
- C. Lee et al., *Plant J.* **99**, 452–464 (2019).
- R. Schwab, S. Ossowski, M. Riester, N. Warthmann, D. Weigel, *Plant Cell* **18**, 1121–1133 (2006).
- S. Jin, Z. Nasim, H. Susila, J. H. Ahn, *Semin. Cell Dev. Biol.* **109**, 20–30 (2020).

ACKNOWLEDGMENTS

We are grateful to J. Browse, C. Benning, and D. Weigel for providing research materials and H. K. Song for fluorescence polarization spectroscopy experiments. We also thank S. J. Yoo, Y. J. Kim, S. M. Hong, and H. Y. Shin for technical assistance.

Funding: This work was supported by a National Research Foundation (NRF) of Korea grant funded by the Korean government (NRF-2017R1A2B3009624 to J.H.A.) and Samsung Science and Technology Foundation (SSTF-BA1602-12 to J.H.A.). This work was also supported by the Singapore National Research Foundation Investigatorship Programme (NRFNRFI2016-02 to H.Y.). **Author contributions:** H.S., S.Ju., and J.H.A. conceived the research direction; H.S. performed most of the experiments; S.Ju. performed preliminary analyses; L.L. and H.Y. performed immunogold transmission electron microscopy; K.G. and M.C.S. performed lipidomics analysis; K.G. performed PG feeding experiments; K.G., K.S.C., and H.S. performed cotyledon grafting; K.S.C., S.Ji., G.Y., and Z.N. generated the transgenic lines; S.-J.K. generated the untagged FT protein; H.S. and J.H.A. analyzed and interpreted data, supervised the project, and wrote the manuscript; and S.Ju., L.L., and H.Y. commented on the manuscript. **Competing interests:** The authors declare no competing interests. **Data and materials availability:** All data are available in the main text or in the supplementary materials.

SUPPLEMENTARY MATERIALS

science.sciencemag.org/content/373/6559/1137/suppl/DC1
Materials and Methods
Figs. S1 to S18
Tables S1 to S3
References (26–66)
MDAR Reproducibility Checklist

[View/request a protocol for this paper from Bio-protocol.](https://bio-protocol.org/View/Request_a_protocol_for_this_paper_from_Bio-Protocol.html)

6 March 2021; accepted 7 July 2021
10.1126/science.abh4054

Florigen sequestration in cellular membranes modulates temperature-responsive flowering

Hendry Susila¹ Snježana Jurić¹ Lu Liu² Katarzyna Gawarecka¹ Kyung Sook Chung¹ Suhyun Jin³ Soo-Jin Kim³ Zeeshan Nasim⁴ Geummin Youn⁵ Mi Chung⁵ Suh Hao⁵ Yu Ji⁵ Hoon Ahn⁵

Science, 373 (6559), • DOI: 10.1126/science.abh4054

Linking flowering to ambient temperature

In the small mustard plant *Arabidopsis*, the florigen FLOWERING LOCUS T (FT) mobilizes to initiate flowering at the shoot apical meristem. Susila *et al.* now show that FT, which is produced in leaf cells, can be held in reserve if ambient temperatures are not favorable (see the Perspective by Jaillais and Parcy). At low temperatures, FT binds a membrane phospholipid and is thus restricted in mobility. At higher temperatures, such binding is less favored, and FT is released to mobilize into the shoot apical meristem to drive flowering. Thus, temperature-sensitive lipid binding helps the plant time flowering with favorable ambient temperatures. —PJH

View the article online

<https://www.science.org/doi/10.1126/science.abh4054>

Permissions

<https://www.science.org/help/reprints-and-permissions>